Phase diagram of the frustrated Heisenberg antiferromagnet on the union jack lattice

Weihong Zheng, J. Oitmaa, and C. J. Hamer
School of Physics, The University of New South Wales, Sydney, NSW 2052, Australia
(Received 29 October 2006; revised manuscript received 28 March 2007; published 17 May 2007)

We use series expansions to investigate the zero-temperature phase diagram of a recently proposed frustrated quantum spin-1/2 antiferromagnet on the two-dimensional union jack lattice with coupling ratio α. A single second-order phase transition is found between a Néel phase and a canted ferrimagnetic phase at a critical coupling $\alpha_c=0.65(1)$. The Néel magnetization vanishes at the transition. Dispersion curves for magnon excitations are also obtained and compared with spin-wave predictions. Two Goldstone modes are found in the canted phase, one linear in momentum and the other quadratic, in accordance with theoretical predictions.

DOI: 10.1103/PhysRevB.75.184418 PACS number(s): 75.10.Jm, 75.30.Ds, 05.30.−d

I. INTRODUCTION

The physics of two-dimensional quantum antiferromagnets on frustrated lattices is surprisingly rich and still not fully understood. Various models have been studied in recent years, including the square lattice J_1-J_2 model[1–3] (a model for Li_2VOSiO_4), the Shastry-Sutherland model[4,5] [a model for $SrCu_2(BO_2)_3$], and the anisotropic triangular lattice[6,7] (a model of Cs_2CuCl_4). Each of these models is based on a square-lattice $S=1/2$ antiferromagnet with nearest-neighbor exchange J_1 and the addition of frustrating second-neighbor exchanges $J_2=\alpha J_1$ on some or all of the plaquettes of the lattice. Although all of these models show antiferromagnetic Néel order for small α, the phase diagrams for larger α appear to differ, showing variously columnar order, spiral order, or dimerization. The rich and sometimes exotic physical phenomena expected in such systems are well described in a recent review.[8]

It is then of interest to investigate other models of this type. One such case is the union jack lattice, shown in Fig. 1. This lattice has been studied in classical statistical mechanics for some time,[9] but has only been considered in the context of quantum antiferromagnets very recently by Collins *et al.*[10] (hereafter referred to as I), who treated the model via spin-wave theory. This approach appeared to predict a first-order phase transition from a Néel phase to a canted ferrimagnetic phase and the existence of two kinds of spin-wave excitations (α and β bosons) with characteristic dispersion features. Spin-wave theory, however, is by no means always reliable for frustrated systems with strong quantum corrections, so it is desirable to test these predictions using a more accurate systematic approach, such as series expansions.[11] That is the motivation behind the present work.

The Hamiltonian for our lattice model is

$$H = J_1 \sum_{\langle ij \rangle} \mathbf{S}_i \cdot \mathbf{S}_j + J_2 \sum_{\langle jk \rangle} \mathbf{S}_j \cdot \mathbf{S}_k, \tag{1}$$

where the interactions are both antiferromagnetic ($J_1, J_2 > 0$), the summations are over the two kinds of bonds shown in Fig. 1, and the $\mathbf{S}_i$ are spin-1/2 operators. In the following we will set $J_1=1$ and $J_2=\alpha J_1=\alpha$.

A classical variational analysis[10] predicts that for $\alpha = J_2/J_1 < 0.5$, the ground state is the Néel state, as in the J_1-J_2 model. For $\alpha > 0.5$, the ground state is the canted ferrimagnetic state shown in Fig. 2, where the spins on the A sublattice are canted at an angle θ to those on the B sublattice and at angle 2θ to their neighbors on the A sublattice, with the angle θ given by

$$\cos\theta = \frac{1}{2\alpha}. \tag{2}$$

In the limit $\alpha \to \infty$, the angle $\theta \to \pi/2$: the spins on the A sublattice are then Néel ordered, as expected, and the spins on the A and B sublattices are at right angles to each other.

The modified second-order spin-wave expansion of I appeared to show that the transition between the Néel and canted phases is postponed until $\alpha_c \simeq 0.84$, with the ground-state energy remaining lowest in the Néel phase out to that point. The staggered magnetization according to this expansion remains substantial at $\alpha \simeq 0.8$, but by analogy with the J_1-J_2 model it was argued[10] that higher-order quantum fluctuations might well reduce the magnetization at larger α and result in a second-order transition. Another intriguing feature of the spin-wave results was the development of an instabil-

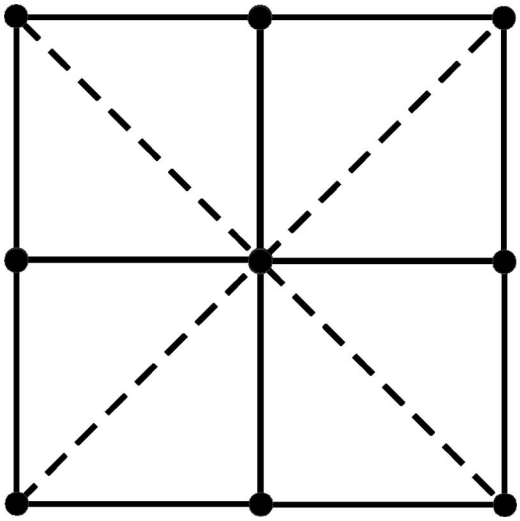

FIG. 1. The Heisenberg spin model on the union jack lattice. Solid lines represent nearest-neighbor antiferromagnetic interactions J_1; dashed lines represent next-nearest-neighbor interactions J_2.

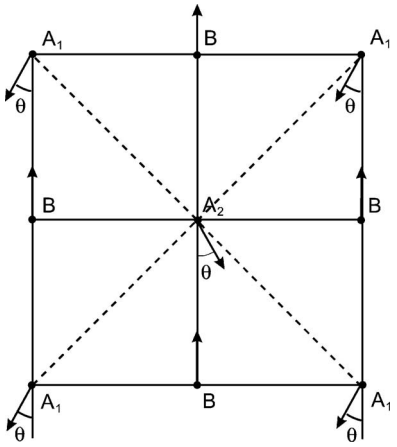

FIG. 2. Spin configurations in the canted phase.

ity in the single-particle dispersion relation at $\alpha=0.65$, with a vanishing energy gap and quadratic dispersion at nearby momenta. This is another indication of a possible second-order transition. More accurate numerical calculations were clearly called for.

The ground state in the canted phase has ferromagnetic order in the z (vertical) direction and antiferromagnetic order in the x (horizontal) direction, as shown in Fig. 2. Thus the O(3) symmetry of the Hamiltonian is completely broken, as it takes two vectors to specify the orientation of the order parameters. The physics of such phases has been discussed by Sachdev and co-workers[12,13] and Roman and Soto,[14] who predict that such a system should possess one linear and one quadratic Goldstone mode. This is consistent with the general counting rules of Nielsen and Chadha,[15] who show that for a nonrelativistic system, if each linear mode is counted once and each quadratic mode is counted twice, then the total number of "bosons" so obtained should be equal to or greater than the number of symmetry generators that are spontaneously broken (3, in this case).

The characteristics of a second-order transition between a canted phase and a Néel phase have been discussed by Sachdev and Senthil[12] using a generic quantum rotor model and assuming that the Néel magnetization and spin-wave stiffness remain finite at the transition point. A renormalization group analysis shows that spatial dimension $d=2$ is the upper critical dimension for such systems, with critical exponents

$$z=2, \quad \eta=0, \quad \nu=1/2, \tag{3}$$

where z is the appropriate dynamic critical exponent. Then using the scaling relation

$$2\beta=(d+z-2+\eta)\nu, \tag{4}$$

we obtain

$$\beta=1/2. \tag{5}$$

In the present work we perform two perturbation series expansions for the model, one in the Néel phase and one in the canted phase. The Néel expansion shows very clear evidence of a continuous second-order phase transition at $\alpha_c \simeq 0.645$, where an extra massless mode with quadratic dispersion develops. The staggered magnetization also vanishes there. The critical exponents can only be crudely estimated, but are roughly given by $\nu=1$, $\beta=1/2$. Thus the transition appears to be in a different universality class from the one discussed by Sachdev and Senthil.[12]

The expansions in the canted phase gives much less accurate results, but they are consistent with a second-order transition at the same point. There is no sign of any intermediate "spin-liquid" phase in between the two ordered phases, such as seems to occur in other two-dimensional frustrated antiferromagnets. The ground-state energy continues smoothly into the canted phase, without any sign of a discontinuity in slope as one would expect at a first-order transition. The canted magnetizations appear to be dropping smoothly towards zero at the critical point, albeit with large error bars. Throughout this phase, the system seems to exhibit two massless Goldstone modes, as predicted by theory.[12–15] There is an unresolved puzzle, however, in that the overall pattern of the magnon dispersion relations seems to be quite different from that predicted by spin-wave theory.

In Sec. II we make some additional remarks on the spin-wave theory discussed in I, and it is shown that the Goldstone modes predicted by general theory are already present in first-order spin-wave theory. In Sec. III we briefly indicate how our series expansions were carried out. Numerical results for the Néel phase are presented in Sec. IV, and for the canted phase in Sec. V. Our conclusions are summarized in Sec. VI.

II. LINEAR SPIN-WAVE THEORY

Spin-wave expansions for this system were discussed in I. One important feature was missed in that discussion, however, which we bring out here: namely, the appearance of the quadratic Goldstone mode. We will use a convention in which k_x and k_y are the components of momentum along the nearest-neighbor axes, and we set the nearest-neighbor spacing to 1, so that the structure constants for the full lattice and the A sublattice are, respectively,

$$\gamma_k=\frac{1}{2}(\cos k_x+\cos k_y),$$

$$\eta_k=\cos k_x \cos k_y. \tag{6}$$

This convention differs from the previous paper, but otherwise, our conventions are the same, and we refer to I for the formalism and further details.

A. Néel phase

Since the Néel state has a two-sublattice structure, the spin-wave excitations (magnons) in this system also have two branches, which we denote the α and β bosons, respectively. According to linear spin-wave theory in the Néel phase, the energy of the α boson in zero magnetic field takes the form [I, Eq. (27)]

$$E_k^{\alpha}=4S\{u_k^2[1-\alpha(1-\eta_k)]+v_k^2-2u_kv_k\gamma_k\}, \tag{7}$$

where S is the spin (here $S=1/2$) and $u_{\mathbf{k}}$ and $v_{\mathbf{k}}$ are given by

$$u_k = \left[\frac{1+h_k}{2h_k}\right]^{1/2}, \quad v_k = \mathrm{sgn}(\gamma_k)\left[\frac{1-h_k}{2h_k}\right]^{1/2}, \tag{8}$$

where

$$h_k = \left(1 - \frac{\gamma_k^2}{f_k^2}\right)^{1/2}, \quad f_k = 1 - \frac{\alpha}{2}(1-\eta_k). \tag{9}$$

We are interested in the special case $\mathbf{k}=(\pi,0)$ [or $(0,\pi)$], where $\gamma_{\mathbf{k}}=0$ and $\eta_{\mathbf{k}}=-1$. Then we find $h_{\mathbf{k}}\to 1$, $u_{\mathbf{k}}\to 1$, and $v_{\mathbf{k}}\to 0$, and $E_{\mathbf{k}}^{\alpha}$ takes the simple form

$$E_{k=(\pi,0)}^{\alpha} = 2[1-2\alpha]. \tag{10}$$

This energy gap vanishes linearly at $\alpha=1/2$, the classical transition point. Beyond this point, the energy eigenvalue at this momentum is negative, and the Néel solution becomes unphysical. In the modified second-order theory, the point at which this gap vanishes moves out to $\alpha_c=0.645$.[10]

B. Canted phase

In linear spin-wave theory for the canted phase, at canting angle θ, the single-particle energies at momenta $(\pm\mathbf{k})$ appear as eigenvalues of the Hamiltonian $H_{\mathbf{k}}$ [I, Eq. (45)]:

$$H_k = 2S[\mathbf{q}_k^{\dagger}\hat{H}_k\mathbf{q}_k + N_k]. \tag{11}$$

Here $\mathbf{q}_{\mathbf{k}}^{\dagger}$ has four components $(a_{\mathbf{k}}^{\dagger}, b_{-k}, b_{\mathbf{k}}^{\dagger}, a_{-\mathbf{k}})$, where $(a_{\mathbf{k}}^{\dagger}, a_{\mathbf{k}})$ and $(b_{\mathbf{k}}^{\dagger}, b_{\mathbf{k}})$ are the usual spin-deviation operators on the A and B sublattices, respectively, with commutation relations among them:

$$[q_i, q_j^{\dagger}] = J_i\delta_{ij} \quad (i,j=1,\ldots,4). \tag{12}$$

Here J is a diagonal matrix with diagonal elements $(1,-1,+1,-1)$. The matrix $\hat{H}_{\mathbf{k}}$ has the form

$$\hat{H}_k = \begin{bmatrix} A & C & D & E \\ C & B & 0 & D \\ D & 0 & B & C \\ E & D & C & A \end{bmatrix}, \tag{13}$$

with

$$A = 2(\cos\theta - \alpha\cos 2\theta) + \alpha(1+\cos 2\theta)\eta_k,$$

$$B = 2\cos\theta,$$

$$C = -(1+\cos\theta)\gamma_k,$$

$$D = (1-\cos\theta)\gamma_k,$$

$$E = -\alpha(1-\cos 2\theta)\eta_k, \tag{14}$$

and the normal-ordering correction is

$$N_k = -A - B. \tag{15}$$

We look for the eigenvalues of $H_{\mathbf{k}}$ under the generalized Bogoliubov transformation

$$q_i = \sum_j S_{ij} q_j' \quad (i,j=1,\ldots,4), \tag{16}$$

$$\hat{H}_k' = S^{\dagger}\hat{H}_k S, \tag{17}$$

which preserves the commutation relations (12); this implies that

$$SJS^{\dagger} = J. \tag{18}$$

Now S is not unitary, and so the eigenvalues of $\hat{H}_{\mathbf{k}}$ are not invariant under the transformation. We note, however, that from Eqs. (17) and (18) it follows that

$$(JS)^{-1}(\hat{H}_k J)(JS) = J\hat{H}_k', \tag{19}$$

and so a similarity transform of $\Delta \equiv \hat{H}_{\mathbf{k}}J$ can be used to produce a diagonal matrix $J\hat{H}_{\mathbf{k}}' = \hat{H}_{\mathbf{k}}'J$, which does preserve eigenvalues.[16] The matrix Δ is given by

$$\Delta = \begin{bmatrix} A & -C & D & -E \\ C & -B & 0 & -D \\ D & 0 & B & -C \\ E & -D & C & -A \end{bmatrix}. \tag{20}$$

The characteristic equation $\det(\Delta - \lambda I)=0$ then yields a quartic equation for the eigenvalues,

$$\lambda^4 - 2b\lambda^2 + c = 0, \tag{21}$$

where

$$b = \frac{1}{2}(A^2 + B^2 - 2C^2 + 2D^2 - E^2),$$

$$c = [B(A-E) - (C-D)^2][B(A+E) - (C+D)^2]. \tag{22}$$

The solutions are

$$\lambda^2 = b \pm \sqrt{b^2 - c} \tag{23}$$

or

$$\omega_k = 2S\sqrt{[b \pm \sqrt{b^2 - c}]} \tag{24}$$

for the eigenvalues of the original Hamiltonian.

Setting $\cos\theta = 1/(2\alpha)$ (the classical value), the various constants can be simplified:

$$b \to \left[\frac{1+4\alpha^4}{\alpha^2} + 2\eta_k + 2(1-2\alpha^2)\eta_k^2 - \frac{4}{\alpha}\gamma_k^2\right] \Big/ 2,$$

$$c \to \frac{2}{\alpha^2}[1+\eta_k - 2\gamma_k^2][2\alpha^2 + (1-2\alpha^2)\eta_k - \gamma_k^2]. \tag{25}$$

Now let us look at some special cases:

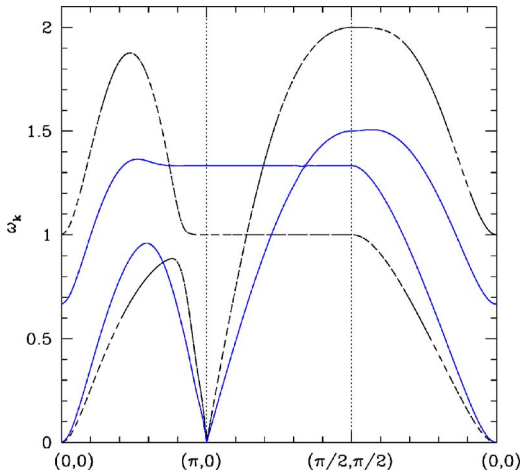

FIG. 3. (Color online) Dispersion relations for the one-particle states for $\alpha=0.75$ (solid lines) and 1 (dashed lines), along high-symmetry cuts in the Brillouin zone, as predicted by linear spin-wave theory in the canted phase.

1. $|\mathbf{k}| \ll 1$

Then $\gamma_{\mathbf{k}} \sim 1-k^2/4$, $\eta_{\mathbf{k}} \sim 1-k^2/2$ and $b \sim (2-1/\alpha)/2$, $c \sim k^4$. Hence the two energies are

$$\omega_k \sim 2S\left(2-\frac{1}{\alpha}\right), \quad \frac{2\alpha S}{2\alpha-1}k^2. \tag{26}$$

Here we see the emergence of an extra quadratic zero mode at zero momentum. At $\alpha=1/2$, the zero mode becomes linear, as in the Néel phase.

2. $\mathbf{k}=(\pi,0)+\mathbf{q}$, $|\mathbf{q}| \ll 1$

Then $\gamma_{\mathbf{k}} \sim q^2/4$, $\eta_{\mathbf{k}} \sim -1+q^2/2$ and $b \sim [1/\alpha^2+(4\alpha^2-1)q^2]/2$, $c \sim (4\alpha^2-1)q^2/\alpha^2$. Hence the two energies are

$$\omega_k \sim \frac{2S}{\alpha}, \quad 2S\sqrt{4\alpha^2-1}|\mathbf{q}|. \tag{27}$$

Here we see the emergence of a *linear* zero mode at $\mathbf{k}=(\pi,0)$. Only at $\alpha=1/2$ does the linear term vanish, and the mode becomes quadratic, matching the result in the Néel phase.

Figure 3 shows a graph of the two energies as functions of $\mathbf{k}$, along high-symmetry cuts in the Brillouin zone, for the cases $\alpha=0.75$ and 1 (note that the numerical results in the canted phase given in I were erroneous, due to a programming error). It can be seen that there is a crossover between the two eigenvalues. The quadratic zero mode at $\mathbf{k}=(0,0)$ and the linear zero mode at $(\pi,0)$ are clearly seen in this figure, satisfying the counting rules of Nielsen and Chadha.[15]

Thus it can be seen that linear spin-wave theory already demonstrates the existence of a massless Goldstone mode with quadratic dispersion, characteristic of a ferromagnetic system, throughout the canted phase. Of course, we expect the dependence of the canting angle θ on α to be renormalized by quantum fluctuation terms at higher order.

III. SERIES EXPANSION METHODS

The method of series expansions is based on dividing the Hamiltonian into two parts $H=H_0+\lambda V$, where H_0 can be solved exactly, λ is a parameter introduced for convenience such that $\lambda=1$ for the physical Hamiltonian, and the V term is treated perturbatively to high order. The resulting series in powers of λ is then evaluated at $\lambda=1$ by standard numerical methods (Padé approximants, integrated differential approximants[11]) to obtain estimates of the physical properties of the original Hamiltonian. The decomposition of H can be done in various ways, depending on the type of phase expected. Details of the approach can be obtained from Ref. 11.

A. Ising expansion in the Néel phase

In the region of small α we expect Néel order, and we use an "Ising expansion"[11] in which H is decomposed as

$$H_0 = \sum_{\langle ij \rangle} S_i^z S_j^z + \alpha \sum_{\langle jk \rangle} S_j^z S_k^z - t \sum_i (S_i^z - 1/2),$$

$$V = \frac{1}{2}\sum_{\langle ij \rangle} (S_i^+ S_j^- + S_i^- S_j^+) + \frac{\alpha}{2}\sum_{\langle jk \rangle} (S_j^+ S_k^- + S_j^- S_k^+) + t\sum_i (S_i^z - 1/2), \tag{28}$$

where S_i^+ and S_i^- are the usual raising and lowering operators, and the sums $\langle ij \rangle$ run over nearest-neighbor pairs, while the sums $\langle jk \rangle$ run over bonds on the A sublattice as shown in Fig. 2. The last term of strength t in both H_0 and V is a local field term, which can be included to improve convergence. The unperturbed ground state is the classical Néel state with energy $E_0/N=-J_1/2+J_2/4$. Series have been obtained to order λ^{13}, at fixed values of α and t, for the ground-state energy per site, the near-neighbor correlation functions $\{\langle S_i^\alpha S_j^\alpha \rangle, \alpha=x,y,z\}$ and the staggered magnetization $M^s=\langle (-1)^i S_i^z \rangle$. This calculation requires 3 070 628 linked clusters of up to 13 sites.

Excitation energies can also be obtained using a linked-cluster expansion.[11,17] We have obtained series for the magnon energy $\omega_{\mathbf{k}}$ to order λ,[10] involving 2 106 181 clusters of up to 11 sites. Results of the analysis are presented in the next section.

B. Ising expansions in the canted phase

We turn now to the large-α phase. The classical ground state is the canted ferrimagnetic state discussed in Sec. I, with canting angle $\cos\theta=1/2\alpha$. Quantum fluctuations will modify this picture to some degree, of course. In linear spin-wave theory, the canting angle is unchanged from the classical result. In the series approach θ is not known *a priori*, and it is necessary to compute series for different values of θ and then determine θ by some criterion, such as minimizing the ground-state energy. This approach has been used previously[6] for the anisotropic triangular lattice.

Following I, we quantize the spins with respect to the axes shown in Fig. 2, so that the z axis on the B sublattice points upwards and the z axes on the sublattices A_1 and A_2

are canted at angle θ to the downwards direction as shown, where θ is a parameter to be determined. The y axes are taken to lie perpendicular to the paper in each case. In terms of spin components, we then write

$$H_0 = -\cos\theta \sum_{B:\mathbf{n},\mu} S^z_{B:\mathbf{n}} S^z_{A:\mathbf{n}+\mu} + \alpha \cos 2\theta \sum_{A1:\mathbf{n},\mu'} S^z_{A1:\mathbf{n}} S^z_{A2:\mathbf{n}+\mu'} - t\sum_i (S^z_i - 1/2) \tag{29}$$

and

$$V = \sum_{B:\mathbf{n},\mu} [-S^x_{B:\mathbf{n}} S^x_{A:\mathbf{n}+\mu} \cos\theta + \eta_{\mathbf{n}\mu}(S^z_{B:\mathbf{n}} S^x_{A:\mathbf{n}+\mu} - S^x_{B:\mathbf{n}} S^z_{A:\mathbf{n}+\mu})\sin\theta + S^y_{B:\mathbf{n}} S^y_{A:\mathbf{n}+\mu}] + \alpha \sum_{A1:\mathbf{n},\mu'} [S^x_{A1:\mathbf{n}} S^x_{A2:\mathbf{n}+\mu'} \cos 2\theta + S^y_{A1:\mathbf{n}} S^y_{A2:\mathbf{n}+\mu'} + (S^z_{A1:\mathbf{n}} S^x_{A2:\mathbf{n}+\mu'} - S^x_{A1:\mathbf{n}} S^z_{A2:\mathbf{n}+\mu'})\sin 2\theta] + t\sum_i (S^z_i - 1/2). \tag{30}$$

Here the direction vectors are $\{\mu\} = \pm\mathbf{i}, \pm\mathbf{j}$ and $\{\mu'\} = \pm(\mathbf{i} \pm \mathbf{j})$ and the phase factor $\eta_{\mathbf{n}\mu} = \pm(-1)^{n_y}$ for μ equals $\pm\mathbf{i}$ or $\pm\mathbf{j}$, respectively. The last term of strength t in both H_0 and V is a local field term, which can be included to improve convergence.

Since the canted state also has a two sublattice structure, the spin-wave excitations (magnons) in this system again have two branches, which we denote as in the previous subsection. In this phase, we have obtained series for the ground-state energy per site, the staggered magnetization in the x and z directions, the net magnetization in the z direction to order λ^{12}, and the one-magnon dispersion to order λ^9.

IV. RESULTS IN THE NÉEL PHASE

A. Ground-state energy

In Fig. 4 we show the ground-state energy as a function of $\alpha = J_2/J_1$ and, for comparison, results from linear and second-order spin-wave theory.[10] The series estimates in the Néel phase lie just slightly higher than the modified spin-wave values. In the canted phase, only linear spin-wave results are available, shown as the solid curve for $\alpha > 0.5$. Anticipating Sec. V, series estimates for the ground-state energy in the canted phase are also shown as open circles in the figure. It can be seen that the estimates from the two series expansions merge at $\alpha \simeq 0.65$, marking the transition point between the two phases. The two curves merge smoothly, without any visible discontinuity in slope, providing a first indication that the transition is second order.

B. Staggered magnetization

Figure 5(a) shows the staggered magnetization in the Néel phase as a function of α, together with the best available spin-wave estimate.[10] It can be seen that the series results agree well with the spin-wave estimates at small α, but then drop away rapidly and vanish at $\alpha \simeq 0.65$. This is an even stronger indicator that we are in the vicinity, at least, of a second-order phase transition. However, the error bars in this region are large and it is not possible, from the series, to obtain the critical point α_c with high accuracy or even to exclude the possibility of a weak first-order transition. The spin-wave estimates substantially overestimate the magnetization at larger α and, hence, the region of stability of the Néel phase.

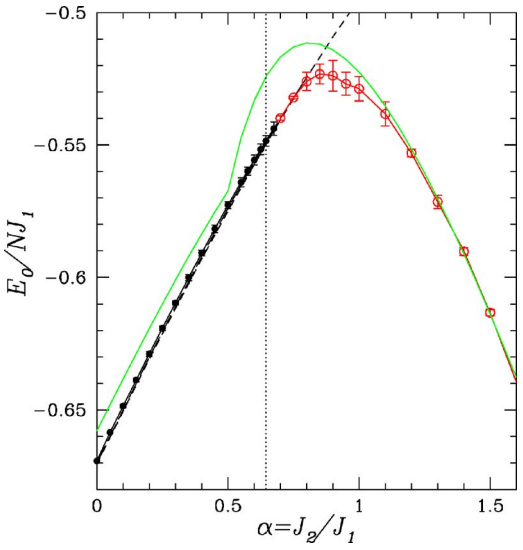

FIG. 4. (Color online) Ground-state energy per site in the Néel and canted phases, from Ising expansions. Also shown are the results from linear spin-wave theory (solid line) and modified second-order spin-wave theory (dashed line) in the Néel phase. The vertical line shows the estimated position of the critical point, at $\alpha_c \simeq 0.65$. To the left of the line the system is in the Néel phase and to the right in the canted phase.

Assuming a second-order transition, a simple fit of the form $M \sim a(\alpha_c - \alpha)^\beta$ in the vicinity of the transition gives a critical point $\alpha_c = 0.65(1)$ and a critical index $\beta = 0.4(1)$, possibly compatible with a square-root branch point, such as the mean-field value predicted by Sachdev and Senthil.[12]

To help delineate the limit of stability of the Néel phase more precisely, we have also derived and analyzed series for the quantity

$$\Delta C = |3\langle S^z_i S^z_j\rangle - \langle \mathbf{S}_i \cdot \mathbf{S}_j\rangle|, \tag{31}$$

which is a measure of the breaking of spin rotational symmetry. At the transition point we expect $O(3)$ spin symmetry to be restored and hence $\Delta C = 0$. Figure 5(b) shows ΔC for the nearest-neighbor and next-nearest-neighbor correlations as functions of α. The transition appears to be second order, with ΔC going continuously to zero and yielding an estimate $\alpha_c = 0.64 \pm 0.02$.

C. Single-particle dispersion

We turn now to the magnon excitations. The dispersion curve obtained from series provides a rather stringent test of the approximate spin-wave theories and also provides estimates of energy gaps and hence of critical points, where the gap vanishes. Figure 6 shows dispersion curves along sym-

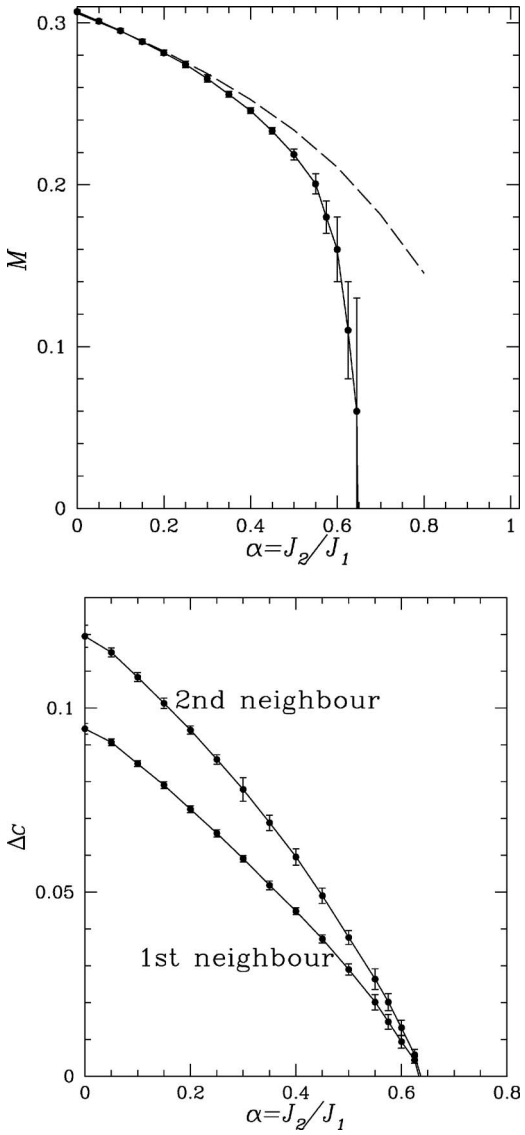

FIG. 5. (a) Staggered magnetization M in the Néel phase from series (circles with error bars), with modified spin-wave estimates (from I) shown as the dashed line. (b) Correlation parameters ΔC [Eq. (31)], for first and second neighbors.

metry lines in the Brillouin zone, for various values of α, in the Néel phase.

Both magnon species are gapless at $\mathbf{k}=(0,0)$, and it is evident that the α-boson branch also becomes gapless at $\mathbf{k}=(\pi,0)$ [and $(0,\pi)$] as α approaches the critical value $\alpha_c \simeq 0.645$, yet further evidence of a second-order transition at that point. The dispersion near the gapless points $(\pi,0)$ and $(0,\pi)$ is quadratic, just as predicted for the critical point by spin-wave theory. There is remarkable agreement with the predictions of the modified second-order spin-wave theory for this dispersion relation. The only discrepancy is the variation between momenta $(\pi,0)$ and $(\pi/2,\pi/2)$: this small discrepancy was already noticed for the simple square-lattice Heisenberg model[18]. Thus spin-wave theory for this quantity remains remarkably accurate even up to the critical point.

Figure 7 shows the energy gap at $\mathbf{k}=(\pi,0)$ as a function of α. The data can be quite well represented by a straight

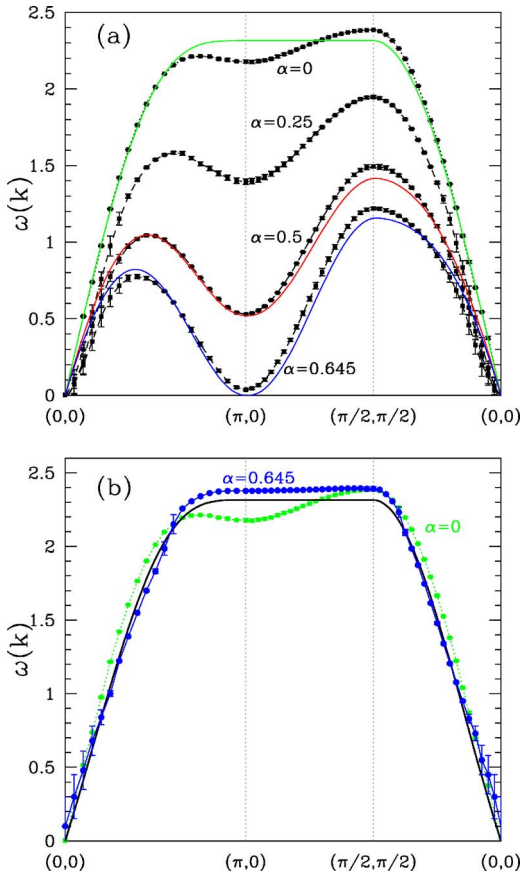

FIG. 6. (Color online) Dispersion curves for (a) the α-boson and (b) β-boson excitations along symmetry lines in the Brillouin zone, for various $\alpha=J_2/J_1$ in the Néel phase. The solid lines are the result of second-order spin-wave theory (Ref. 10).

line, corresponding to a critical index $\nu=1$ and a critical point $\alpha_c=0.656(5)$.

The dispersion of the β bosons does not vary greatly with α, as was already seen in spin-wave theory.

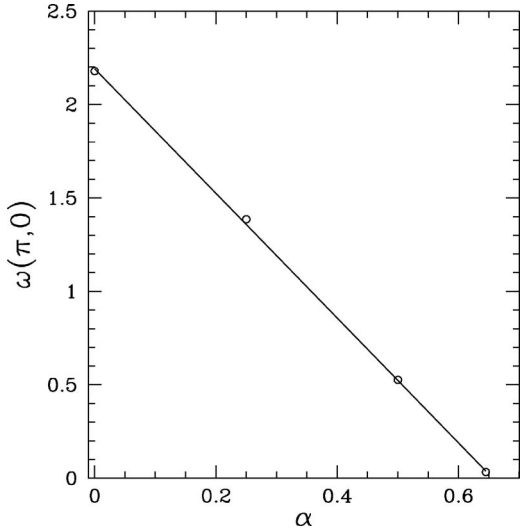

FIG. 7. The energy gap at $\mathbf{k}=(\pi,0)$ as a function of α. The straight line is a least-squares fit to the data. The gap vanishes at $\alpha_c=0.656(5)$.

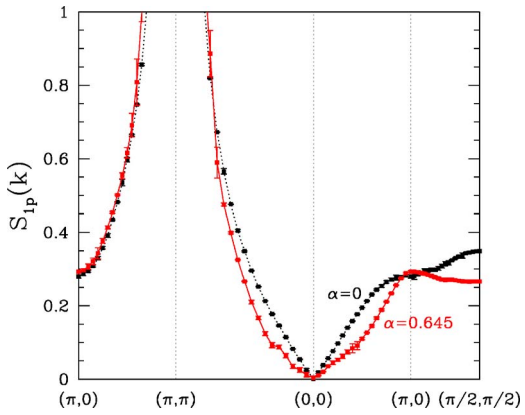

FIG. 8. (Color online) One-particle transverse spectral weight for the α boson.

D. Single-particle spectral weight

Figure 8 shows the α-boson transverse spectral weight $S_{1p}(\mathbf{k})$ along high-symmetry cuts in the Brillouin zone, where $S_{1p}(\mathbf{k})$ is the single-particle contribution to the transverse structure factor

$$S(\omega,\mathbf{k}) = \frac{1}{2\pi N}\sum_{i,j}\int_{-\infty}^{\infty} e^{i[\omega t+\mathbf{k}\cdot(\mathbf{r}_i-\mathbf{r}_j)]}\langle S_j^x(t)S_i^x(0)+S_j^y(t)S_i^y(0)\rangle dt$$
$$= \delta(\omega-\Delta(\mathbf{k}))S_{1p}(\mathbf{k})+\cdots . \quad (32)$$

It can be seen that the overall spectral weight changes remarkably little between $\alpha=0$ and $\alpha=0.645$. As in the square lattice Heisenberg model,[11] the spectral weight vanishes at $\mathbf{k}=(0,0)$ and diverges at $\mathbf{k}=(\pi,\pi)$. Note that it remains *finite* at $\mathbf{k}=(\pi,0)$, even at the critical point. Normally, one expects the one-particle spectral weight to diverge as the energy gap vanishes at a critical point,[19] so in this case the quasiparticle residue must vanish at the critical point. This is consistent with the general behavior of Goldstone bosons, whose couplings are "soft"—i.e., vanish at zero momentum.

The series for the structure factor of the β boson does not converge well, and we display no results for it here.

V. RESULTS IN THE CANTED PHASE

We turn now to the canted phase at large α. It is harder to obtain accurate results here than it is in the Néel phase. The expansions are technically more complicated since we need to divide the lattice into four sublattices, and so the expansion cannot be carried to such high orders, and to this must be added the uncertainty in the canting angle θ. The value of θ was determined in the following manner. We expect a zero mode to develop at $\mathbf{k}=(\pi,0)$ in the canted phase, and the estimated energy gap at this momentum turns out to be particularly sensitive to the value of θ. Thus we searched for a value of θ where the estimated energy gap at this point does in fact vanish. The canting angle is determined quite accurately by this criterion. Figure 9 shows the behavior of the canting angle as a function of α, together with the classical prediction $\cos\theta=1/2\alpha$. The series result lies substantially lower than the classical one at all values of α.

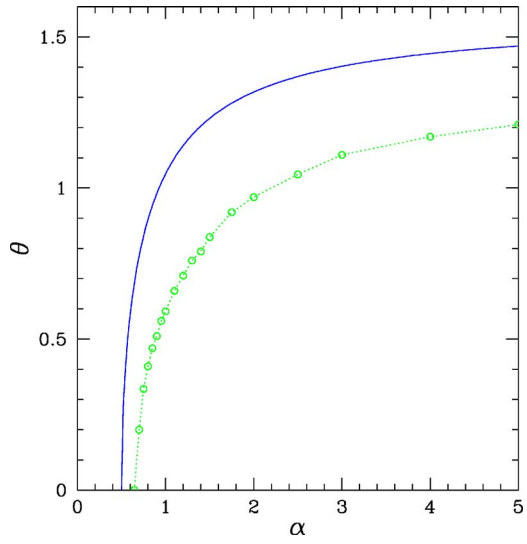

FIG. 9. (Color online) Estimated canting angle in the canted phase as a function of α. The solid line is the classical result $\cos\theta=1/2\alpha$, while the circles are the series estimates.

The ground-state energy in this phase has already been discussed in Sec. IV A. It is not very sensitive to the estimate of θ.

A. Magnetizations

Figures 10(a), 10(b), and 10(c) show estimates of the average magnetization $M_z=\langle S^z\rangle$ in the z direction, the staggered magnetization in the z direction, $M_z^s=\langle(-1)^{x+y}S^z\rangle$, and the staggered magnetization in the x direction, $M_x^s=\langle(-1)^y S^x\rangle$, respectively, as functions of α. All of them appear to be trending downwards towards zero at the critical point $\alpha=0.65$ but the errors in these estimates are rather large, and it is hardly possible to extract meaningful estimates of the critical exponents.

B. Single-particle dispersion

Figures 11(a) and 11(b) show the dispersion relations of the α and β bosons, respectively, at some representative couplings. The results here are rather different from the linear spin-wave predictions. The α-boson energy remains finite at $\mathbf{k}=(0,0)$ and vanishes at $(\pi,0)$, as we required when fixing θ, but the behavior in the neighborhood of the zero mode appears to be quadratic in momentum, rather than linear as predicted by the spin-wave theory. The β boson, on the other hand, has a zero mode at $\mathbf{k}=(0,0)$ which appears to be linear rather than quadratic. Thus the counting rules of the general theory are satisfied, but the linear and quadratic modes appear to be *interchanged* as compared with the spin-wave prediction.

Further evidence comes from the behavior of the energy gap as a function of λ, the anisotropy parameter. A standard D log Padé analysis (Table I) was made to estimate the critical exponent of the gap as a function of λ. For the α boson at $(\pi,0)$, the exponent is very close to 1, corresponding to a linear zero at $\lambda=1$, while for the β boson at (0, 0), it is very

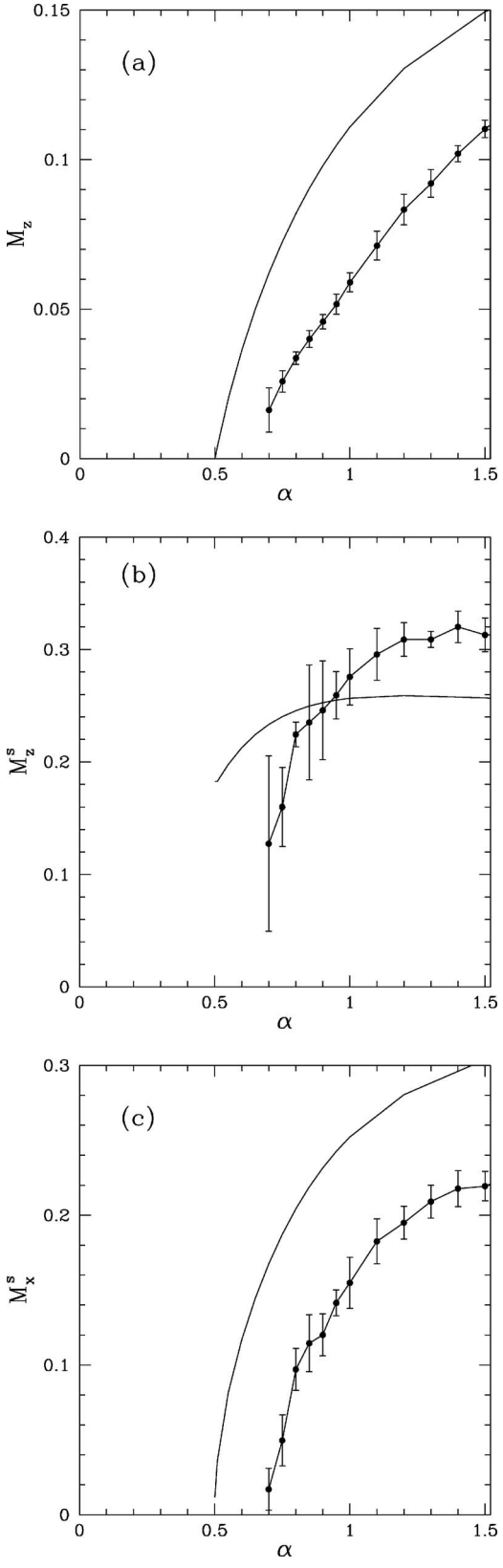

FIG. 10. Estimates of (a) the average magnetization $M_z=\langle S^z\rangle$ in the z direction, (b) the staggered magnetization in the z direction, $M_z^s=\langle(-1)^{x+y}S^z\rangle$, and (c) the staggered magnetization in the x direction, $M_x^s=\langle(-1)^y S^x\rangle$, as functions of α. The solid curves are the linear spin-wave results.

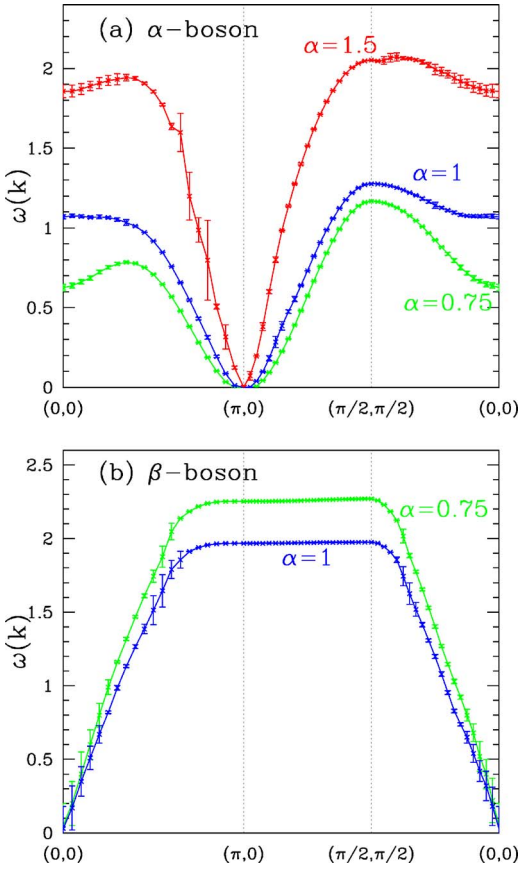

FIG. 11. (Color online) Dispersion curves for (a) α-boson and (b) β-boson excitations for various $\alpha=J_2/J_1$ in the canted phase of the union jack model. The solid lines are merely to guide the eye.

close to 0.5, indicating a square-root branch point. Now in spin-wave theory, an exponent 0.5 is associated with linear behavior in momentum, while an exponent of 1 would be associated with quadratic behavior in momentum. It can be shown that the same connection holds for this model, at least in leading order of spin-wave theory. These results reinforce the momentum dependence outlined above. The complicated crossover between α and β bosons predicted by linear spin-wave theory also does not seem to occur in the series results.

VI. SUMMARY AND CONCLUSIONS

We have used both high-order series expansions and spin-wave theory to explore the phase diagram of a frustrated Heisenberg spin model on the union jack lattice.

Series expansions in the Néel phase at small couplings α show very clear evidence of a second-order phase transition at a critical coupling $\alpha_c=0.65(1)$. Both the staggered magnetization and the energy gap at momentum $\mathbf{k}=(\pi,0)$ vanish at that point. The magnon dispersions in this phase are remarkably close to the predictions of the modified spin-wave theory. The critical indices can only be crudely estimated, but are consistent with $\nu=1$, $\beta=1/2$.

For couplings $\alpha>\alpha_c$, the system lies in the canted phase predicted by the classical theory.[10] There is no sign of any intermediate "spin-liquid" phase between the two ordered

TABLE I. Pole (residue) of $[N/M]$ Dlog Padé approximants to the α-boson gap as a function of λ at $\mathbf{k}=(\pi,0)$ and the β-boson gap at $\mathbf{k}=(0,0)$ for $\alpha=1$, $\theta=0.592$, and $t=1$. Defective approximants are marked with an asterisk.

	$N-2/N$	$N-1/N$	N/N	$N+1/N$	$N+2/N$
			α-boson gap at $\mathbf{k}=\pi,0$, unbiased		
$N=1$		1.0277(1.282)	1.1044(1.481)	1.0800(1.385)	1.0087(1.054)
$N=2$	1.1111(1.509)	1.0858(1.413)	1.1152(1.504)*	0.9363(0.677)	0.9655(0.841)
$N=3$	1.1361(1.562)*	1.0120(1.126)	0.9776(0.922)	1.0494(1.563)	0.9857(0.966)
$N=4$	0.9795(0.935)	0.9926(1.021)	0.9928(1.023)		
$N=5$	0.9928(1.023)				
			α-boson gap at $\mathbf{k}=\pi,0$, biased $\lambda_c=1$		
$N=1$			1.0000(1.214)	1.0000(1.099)	1.0000(1.018)
$N=2$	1.0000(1.215)	1.0000(1.262)*	1.0000(0.818)	1.0000(1.008)	1.0000(1.016)
$N=3$	1.0000(0.885)	1.0000(1.070)	1.0000(1.056)	1.0000(1.093)	1.0000(1.071)
$N=4$	1.0000(1.057)	1.0000(1.065)	1.0000(1.077)	1.0000(1.083)	
$N=5$	1.0000(1.077)	1.0000(1.426)*			
			β-boson gap at $\mathbf{k}=0,0$, unbiased		
$N=1$		0.4958(0.186)	0.8744(0.580)	1.2308(1.617)	1.4345(2.984)
$N=2$	0.5724(0.000)*	0.9017(−0.095)*	1.6917(−1.361)*	1.3653(2.370)	1.4597(3.187)*
$N=3$	0.9343(0.444)	1.1514(0.998)	0.8865(0.223)	1.2583(1.665)*	1.3423(2.285)*
$N=4$	1.0573(0.679)	1.1114(0.860)	1.5174(5.317)*		
$N=5$	1.0178(0.594)*				
			β-boson gap at $\mathbf{k}=0,0$, biased $\lambda_c=1$		
$N=1$			1.0000(0.758)	1.0000(0.867)	1.0000(0.705)
$N=2$	1.0000(−21.9)*	1.0000(0.911)	1.0000(0.802)	1.0000(1.388)*	1.0000(0.204)
$N=3$	1.0000(0.538)	1.0000(0.576)	1.0000(0.469)	1.0000(0.515)	1.0000(0.341)
$N=4$	1.0000(0.551)	1.0000(0.502)	1.0000(0.473)	1.0000(1.136)*	
$N=5$	1.0000(0.567)*	1.0000(0.555)*			

phases, such as occurs in other frustrated systems. Series expansions in the canted phase give a ground-state energy which continues smoothly from the Néel into the canted phase. The canted ferromagnetic and antiferromagnetic order parameters, in the pattern shown in Fig. 2, appear to drop smoothly towards zero around α_c, albeit with large error bars.

The critical indices estimated at the transition do not agree with those predicted by Sachdev and Senthil[12] for a Néel–to–canted–phase transition. Those authors assumed that the Néel order parameter and spin stiffness would remain finite at the transition, whereas in the present case they vanish. Presumably this places our transition in a different universality class. It would be interesting to see if their methods could be adapted to this case.

Results for the magnon dispersions in the canted phase are consistent, having chosen the appropriate canting angle, with the presence of two Goldstone modes, one linear in momentum near the Goldstone zero and the other quadratic. This accords with theoretical predictions,[12–15] as discussed in the Introduction. However, the pattern of the dispersion curves found by series expansions is quite different from that predicted by spin-wave theory, and the positions of the linear and quadratic Goldstone modes appear to be *interchanged*. Spin-wave theory fails to predict the vanishing of the Néel magnetization at the transition and cannot be taken as an infallible guide, but still this discrepancy remains something of a puzzle.

There is no experimental realization of this model at present, but the ingenuity of physical chemists could possibly provide one in the future. Theoretically, the model is interesting because it exhibits a canted ferrimagnetic phase and a continuous transition from the Néel phase to the canted phase, whose nature deserves further exploration.

ACKNOWLEDGMENTS

We would like to thank Alex Collins for help with some of the calculations. This work forms part of a research project supported by a grant from the Australian Research Council. We are grateful for the computing resources provided by the Australian Partnership for Advanced Computing (APAC) National Facility and by the Australian Centre for Advanced Computing and Communications (AC3).

[1] P. Chandra, P. Coleman, and A. I. Larkin, Phys. Rev. Lett. **64**, 88 (1990).
[2] O. P. Sushkov, J. Oitmaa, and W-H. Zheng, Phys. Rev. B **63**, 104420 (2001).
[3] L. Capriotti, F. Becca, A. Parola, and S. Sorella, Phys. Rev. Lett. **87**, 097201 (2002).
[4] A. Koga and N. Kawakami, Phys. Rev. Lett. **84**, 4461 (2000).
[5] W-H. Zheng, J. Oitmaa, and C. J. Hamer, Phys. Rev. B **65**, 014408 (2002).
[6] W-H. Zheng, J. O. Fjaerestad, R. R. P. Singh, R. H. McKenzie, and R. Coldea, Phys. Rev. Lett. **96**, 057201 (2006).
[7] L. Capriotti, A. E. Trumper, and S. Sorella, Phys. Rev. Lett. **82**, 3899 (1999).
[8] G. Misguich and C. Lhuillier, in *Frustrated Spin Systems*, edited by H. T. Diep (World Scientific, Singapore, 2005).
[9] T. C. Choy and R. J. Baxter, Phys. Lett. A **125**, 365 (1987), and references therein.
[10] A. Collins, J. McEvoy, D. Robinson, C. J. Hamer, and Z. Weihong, Phys. Rev. B **73**, 024407 (2006); **75**, 189902(E) (2007). We note that due to an unfortunate programming error, all the 'linear' spin-wave numerical estimates in this paper are erroneous, in both the Néel and canted phases. The modified second-order spin-wave estimates still stand, however. Corrected estimates are given in the present paper.
[11] J. Oitmaa, C. J. Hamer, and Zheng Weihong, *Series Expansion Methods for Strongly Interacting Lattice Models* (Cambridge University Press, Cambridge, England, 2006).
[12] S. Sachdev and T. Senthil, Ann. Phys. (N.Y.) **251**, 76 (1996).
[13] S. Das Sarma, S. Sachdev, and L. Zheng, Phys. Rev. B **58**, 4672 (1998).
[14] J. M. Roman and J. Soto, Phys. Rev. B **62**, 3300 (2000).
[15] H. B. Nielsen and S. Chadha, Nucl. Phys. B **105**, 445 (1976).
[16] C. Tsallis, J. Math. Phys. **19**, 277 (1978).
[17] M. P. Gelfand, Solid State Commun. **98**, 11 (1996).
[18] Weihong Zheng, J. Oitmaa, and C. J. Hamer, Phys. Rev. B **71**, 184440 (2005).
[19] S. Sachdev, *Quantum Phase Transitions* (Cambridge University Press, Cambridge, England, 1999).